Multi-Resolution Feature Embedded Level Set Model for Crosshatched Texture Segmentation

Original Scientific Paper

Prabhakar K.
Ballari Institute of Technology and Management,
Department of Electronics and Communication Engineering,
Near Allipur, Ballari-583104, India
prabhakar@bitm.edu.in

Sadyojatha K.M.
Ballari Institute of Technology and Management,
Department of Electronics and Communication Engineering,
Near Allipur, Ballari-583104, India
sadyojatha@bitm.edu.in

Abstract *– In image processing applications, texture is the most important element utilized by human visual systems for distinguishing dissimilar objects in a scene. In this research article, a variational model based on the level set is implemented for crosshatched texture segmentation. In this study, the proposed model's performance is validated on the Brodatz texture dataset. The cross-hatched texture segmentation in the lower resolution texture images is difficult, due to the computational and memory requirements. The aforementioned issue has been resolved by implementing a variational model based on the level set that enables efficient segmentation in both low and high-resolution images with automatic selection of the filter size. In the proposed model, the multi-resolution feature obtained from the frequency domain filters enhances the dissimilarity between the regions of crosshatched textures that have low-intensity variations. Then, the resultant images are integrated with a level set-based active contour model that addresses the segmentation of crosshatched texture images. The noise added during the segmentation process is eliminated by morphological processing. The experiments conducted on the Brodatz texture dataset demonstrated the effectiveness of the proposed model, and the obtained results are validated in terms of Intersection over the Union (IoU) index, accuracy, precision, f1-score and recall. The extensive experimental investigation shows that the proposed model effectively segments the region of interest in close correspondence with the original image. The proposed segmentation model with a multi-support vector machine has achieved a classification accuracy of 99.82%, which is superior to the comparative model (modified convolutional neural network with whale optimization algorithm). The proposed model almost showed a 0.11% improvement in classification accuracy related to the existing model*

Keywords: *crosshatched texture, level set, morphological processing, multiresolution, texture segmentation*

1. INTRODUCTION

In image processing applications, texture is a fundamental property of object surfaces and is extensively present in natural images [1-2]. It has an extensive range of applications like texture classification [3-4], spectral shape retrieval video recognition [5], and retrieval [6-7]. Among these available topics, texture classification is an active research area, where it has gained more attention among the researcher's communities in the field of pattern recognition [8] and computer vision [9]. The typical applications of texture classification comprise object recognition, content-based image retrieval, fabric inspection, remote sensing, and medical image analysis [10-12]. On the other hand, the purpose of texture segmentation is to discriminate between the regions, which have dissimilar textures [13]. The texture segmentation is done by using two major methods such as filter bank methods and statistical-based methods [14-15]. The existing methods are implemented by applying the bank of filters to the image, and the filter response is studied to set the image's local behavior. The existing methods' performance completely depends on the texture, which has distinctive statistical properties [16-17].

This research article aims to segment the crosshatched textures and to automate the filter size in order to enhance the dissimilarity between regions with low-intensity variations. Hence, the filter size must be selected cautiously, because when the filter size is large, it causes uncertainties across the boundary regions and if small, then perhaps, it fails to confine certain variations in a few textures. The accurate descriptor and exact filter size are the necessary attributes for good texture segmentation. The main contributions are listed as follows:

- Used histogram equalization technique that improves the contrast of the collected images, which are acquired from the Brodatz texture dataset.
- Developed a precise model for the automatic selection of the filter size. Further, the texture segmentation for crosshatched texture images is done in an unsupervised way. The multi-resolution feature embedded level set model is proposed for texture segmentation.
- The experimental results are validated by using different evaluation measures known as the IoU index, precision, f1-score, recall and accuracy. The segmentation results of the proposed model are compared with the Mix-Normalized-Cut (MixNCut) model, and the classification results are compared with the modified Convolutional Neural Network (CNN) with Whale Optimization Algorithm (WOA). The proposed segmentation model obtains near-perfect accuracy on all crosshatched texture images acquired from Brodatz texture dataset. The proposed model effectively sorts image data into interpretable information and it is utilized in an extensive range of applications like remote sensing, and medical imaging. Industrial application, image retrieval, etc.

This research article is organized as follows: research papers related to texture image segmentation and classification are surveyed in Section 2. The mathematical and theoretical explanation of the proposed model are specified in Section 3. The experimental outcomes of the proposed model is stated in Section 4, and the conclusion of this work is mentioned in Section 5.

2. LITERATURE SURVEY

Maskey and Newman [18] developed a novel texture directionality measure, wherein both global and local directionality aspects were considered. In this literature study, the developed texture directionality measure was employed in different applications that included a circuit board image classification task, striped shirt classification, striped fabric classification and a CNN initialization task. The extensive experimental analysis stated that the suggested measure was superior than the then-existing measures. However, a higher-end graphics processing unit system was required to perform the classification tasks, which proved to be computationally expensive. Ranganath et al. [19] implemented a new image texture classification model named pixel range calculation. As per the derived results, the developed model not only provided superior classification results but also consumed limited computational time related to the conventional models. However, the developed model was ineffective in multi-class texture classification on larger datasets. Dixit et al. [20] integrated a modified CNN model with WOA for effective texture classification. The inclusion of WOA made CNN more effective and robust in texture classification by the selection of optimal parameters. As specified earlier, the implementation of the deep learning models was computationally expensive compared to other machine learning models.

Hilal et al. [21] implemented a new bi-dimensional entropy-based measure for texture classification that included multi-channel methods (FuzEnM2D and FuzEnV2D), and single channel method (FuzEnC2D). The extensive experimental results demonstrated that the developed measure outperformed the well-known texture analysis measures, but the computational time was higher, which needed to be reduced as part of a future extension. Raja et al. [22] developed a new descriptor called Optimized Local Ternary Pattern (OLTP) for effective texture classification. In this literature study, the developed descriptor's effectiveness was validated on two standard datasets namely, Usptex and Brodatz. The obtained simulation outcomes demonstrated that the use of OLTP descriptors effectively improved the texture classification accuracy. However, the developed OLTP descriptor applied only to the gray-scale images, which was considered a major concern in this study. Soares et al. [23] introduced a new class-independent method for segmenting the texture regions from the images. However, the developed method was restricted to a limited number of dissimilar texture classes in the images.

Khan et al. [24] implemented a new descriptor, Overlapped Multi-oriented Triscale Local Binary Patterns (OMTLBP) that effectively retains image classification accuracy under different conditions like illumination, scale, and orientation. In addition to this, Pan et al. [25] developed a new descriptor: Scale-Adaptive LBP (SALBP) for effective texture classification. The effectiveness of the developed OMTLBP and SALBP descriptors was validated on different online datasets like Outex, Brodatz, etc. The obtained experimental outcomes demonstrated the superiority of the developed OMTLBP and SALBP descriptors against traditional texture descriptors using classification accuracy. However, the developed OMTLBP and SALBP descriptors included the concern of high computational time. Feng et al. [26] implemented a new objective measure based on the smallest univalue segment assimilating nucleus method for multi-focus image fusion. By inspecting experimental results, the high computational time was a major issue in this literature. To address the above-mentioned problems, a new multi-resolution feature embedded level set model is implemented for crosshatched texture segmentation.

3. METHODOLOGY

In recent decades, the possibility of inaccurate segmentation is high, when the parameters are selected at the stage of feature extraction or the stage of segmentation voluntarily. Additionally, the supervised texture segmentation schemes require a priori knowledge, and it may not be viable to provide information regarding the number of texture regions and the type of textures to be segmented. Particularly, if the volume of images to be handled is large viz thousands of images in art galleries, large numbers of satellite imagery, etc. [27-30]. The supervised texture segmentation techniques are difficult to provide the prior knowledge manually, and this has motivated the present researchers to look for fully automated schemes. In this research article, an automated model named Multi-Resolution Feature Embedded Level Set Model is implemented for effective crosshatched texture segmentation.

3.1. DATASET DESCRIPTION

In this research article, the proposed multi-resolution feature embedded level set model's performance is evaluated on the Brodatz texture dataset. In text classification, the Brodatz texture dataset is one of the popular datasets, which is recorded from the University of Southern California. The original dataset has rotated images, which are generated by using simple computer-graphics methods. The statistical contribution of the Brodatz texture dataset is denoted in Table 1. The sample images from Brodatz texture dataset are indicated in Fig. 1.

Table 1. Statistical contribution of the Brodatz texture dataset

Features	Values
Size	1.02 GB
Image format	8-bit gray-scale images
Texture patch size	640×640 pixels
Total number of samples	4480
Number of classes with unique samples	40
Number of classes	112

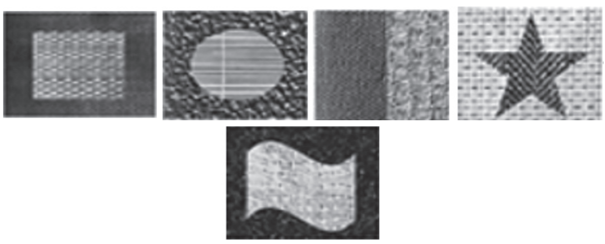

Fig. 1. Sample images of the Brodatz texture dataset

3.2. PRE-PROCESSING

After acquiring the images from Brodatz texture dataset, the image pre-processing is carried out by using a histogram equalization technique that adjusts the crosshatch image intensities for improving the contrast of the images. Let f be considered as the crosshatch image, which is denoted by a matrix integer pixel intensities m, that ranges between 0 to L-1. The histogram equalized crosshatch image g is mathematically determined in equation (1).

$$g_{i,j} = floor\ (L-1)\sum_{n=0}^{f(i,j)} p_n \tag{1}$$

Where, p represents the normalized histogram value of crosshatch image f with a bin-possible intensity, L indicates the intensity value of range 256, and the term floor() rounds off the nearest integers, which are equivalent in transforming the pixel intensity value k, and it is mathematically denoted in equation (2).

$$T(k) = floor(L-1)\sum_{n=0}^{k} p_n \tag{2}$$

The pixel intensities f and g are considered as the continuous random values of X=Y on [0, L-1] in the transformation section, which is mathematically defined in equation (3).

$$Y = T(X) = (L-1)\int_0^x p_X\,(x)dx \tag{3}$$

Where T indicates the cumulative distributive function of X multiplied by L-1 and p_X represents the probability density function of crosshatch image f. In addition to this, Y is represented by $T(X)$, which is uniformly distributed on [0 ,L-1] namely $p_Y\,(y)$=1/(L-1), and it is mathematically defined in equations (4), (5), and (6).

$$\int_0^y p_Y(z)dz = \frac{1}{L-1} = \int_0^{T^{-1}(y)} p_X(w)dw \tag{4}$$

$$\frac{d}{dy}\left(\int_0^y p_Y(z)dz\right) = p_Y(y) = p_X(T^{-1}(y))\frac{d}{dy}(T^{-1}(y)) \tag{5}$$

$$\frac{dT}{dx}_{|x=T^{-1}(y)}\frac{d}{dy}\left(T^{-1}(y)\right) = (L-1)p_X\left(T^{-1}(y)\right)\frac{d}{dy}\left(T^{-1}(y)\right) = 1 \tag{6}$$

where, $p_Y\,(y)$=1/(L-1).

3.3. AUTOMATIC COMPUTATION OF THE FILTER SIZE

In image processing applications, the textures are complicated visual patterns poised on sub-patterns, which show signs of orientation, color, slope, size, etc. For significant texture segmentation, the image features and the selection of the filter size play an important role. Hence, the filter size has to be chosen carefully, since it is capable of capturing the pattern fully, and yields identical values when repeated over the entire homogeneous region.

In this article, an algorithm is developed for the automatic computation of the filter size, and the steps involved are listed below:

- Divide the test crosshatch image into n number of partitions of equal size (size is normally chosen as 21×21, which is usually found to be sufficiently large for the study made on all the textures in Brodatz dataset) and compute the mean of each partition.
- Every partition starts with a smaller filter size of 3×3. Increase the size of the filter until the mean of the filter equals the mean of the partition.

- Group the obtained filter sizes into two clusters.
- Compute mean value of the lower cluster and use it as the filter size.

The method used here involves the computation of a minimum filter size. It is a simple technique in which the filter size is progressively increased until the average within the filter, and average of the partition, are both similar. It ensures that for every region, a maximum filter size is estimated which covers the maximum homogeneous area within that region. The minimum average size among all such regions is selected as the filter size. The algorithm presented above computes the size of the filter involuntarily and is then segmented using a level set. The flowchart of the automated filter selection is indicated in Fig. 2.

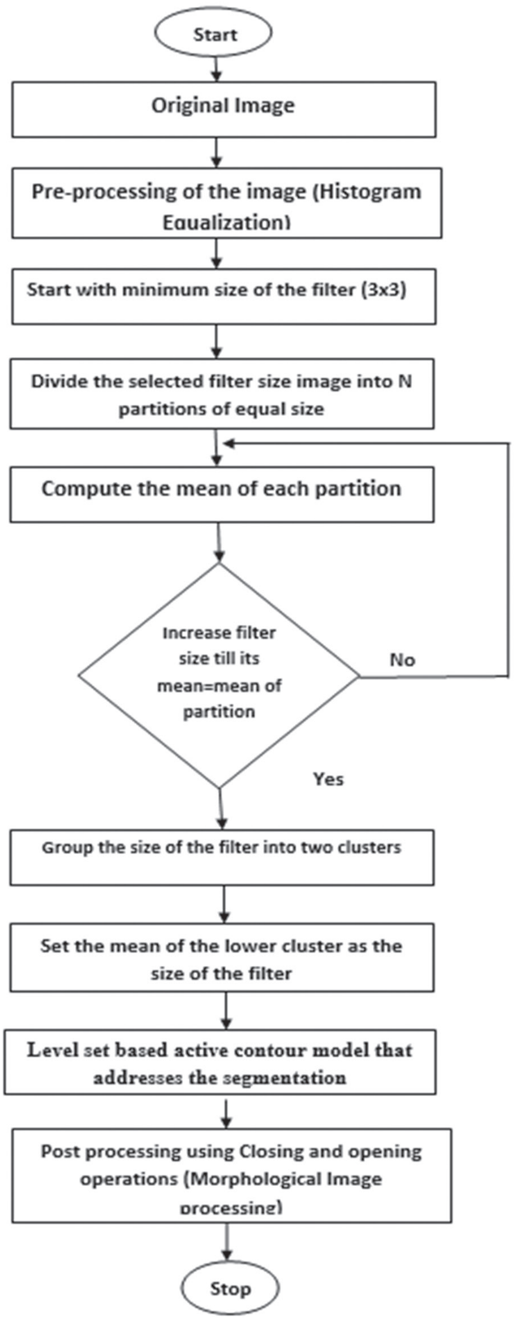

Fig. 2. Flowchart of the automated filter selection

In this article, an algorithm is developed for the automatic computation of the filter size, and the steps involved are listed below:

- Divide the test crosshatch image into n number of partitions of equal size (size is normally chosen as 21×21, which is usually found to be sufficiently large for the study made on all the textures in Brodatz dataset) and compute the mean of each partition.
- Every partition starts with a smaller filter size of 3×3. Increase the size of the filter until the mean of the filter equals the mean of the partition.

- Group the obtained filter sizes into two clusters.
- Compute mean value of the lower cluster and use it as the filter size.

The method used here involves the computation of a minimum filter size. It is a simple technique in which the filter size is progressively increased until the average within the filter, and average of the partition, are both similar. It ensures that for every region, a maximum filter size is estimated which covers the maximum homogeneous area within that region. The minimum average size among all such regions is selected as the filter size. The algorithm presented above computes the size of the filter involuntarily and is then segmented using a level set. The flowchart of the automated filter selection is indicated in Fig. 2.

3.4. MULTI-RESOLUTION FEATURE EMBEDDED LEVEL SET MODEL

In the proposed model, the preprocessed crosshatch image is constructed with two different crosshatched textures that have subjective boundaries. After preprocessing, the next step is selecting the correct size of the frequency domain filter, which is automated. The results obtained are integrated with a level set based active contour model that addresses the segmentation of crosshatched texture images. Any noise incurred during histogram equalization is eliminated by a post-processing step, using morphological processing. The automation process of the frequency domain filters is represented below. Initially it starts with the mean calculation of the filter, which is graphically shown in Fig. 3.

5	3	6
2	1	9
8	4	7

(a)

*	*	*
*	5	*
*	*	*

(b)

Fig. 3. (a) 3×3 Image, and (b) result of the mean filter applied to 3×3 Image

Fig. 3(a) shows a 3×3 image with a center pixel value of 1. Fig. 3(b) shows the mean filter with a center pixel value of 5. The mean filter is a simple sliding-window spatial filter that replaces the center value in a window with the average (mean) of all the pixel values. An example of mean filtering of a single 3×3 window of values is shown in Fig. 3. The filter size is decided interactively by starting with a minimum possible size of 3×3, gradually increasing the size, and continuing the size of the filter until the mean of the pixels within the area is similar. It is important to select the correct filter size for proper segmentation.

The original image is divided into n number of partitions of equal size (the size of the image is normally chosen as 21×21, which is found to be sufficiently large on all the textures in Brodatz dataset), and computes the mean of each partition. Every partition starts with a smaller filter size of 3×3, which is placed at the center of the partition, and then increases the size of the filter until the mean of the filter equals the mean of the partition. The size of the filter obtained is to be grouped into two clusters. The mean value of the lower cluster is used as the filter size. Thus, the obtained automated filtered image is considered for segmentation using a level set.

4. EXPERIMENTAL RESULTS AND DISCUSSION

In this research article, the proposed multi-resolution feature embedded level set model is implemented utilizing a Matlab software environment. An extensive experimental analysis is performed on a computer with an Intel core i5-6200U computer processing unit, an 8 GB Random Access Memory, and a Linux operating system. The segmentation performance of the proposed multi-resolution feature embedded level set model is analyzed using an evaluation measure by name of IoU index. It is a statistical measure used for gauging the similarity and diversity of sample sets, where A and B indicate ground truth and segmented regions. It is mathematically stated in equation (7).

$$I(A,B) = \frac{|A \cap B|}{|A \cup B|} = \frac{|A \cap B|}{|A|+|B|-|A \cap B|} \tag{7}$$

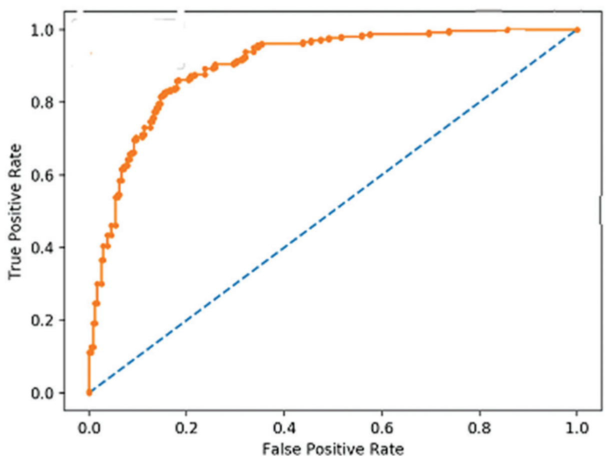

Fig 4. ROC curve of the proposed model

On the other hand, the classification performance of the proposed multi-resolution feature embedded level set model is validated using evaluation measures like accuracy, recall, precision and f1-score, which are stated in equations (8), (9), (10) and (11). True Positive is denoted as (TP), False Positive as (FP), True Negative as (TN), and False Negative as (FN). Meanwhile, the Receiver Operating Characteristic (ROC) curve of the proposed model is stated in Fig 4.

$$Accuracy = \frac{TP+TN}{TP+TN+FP+FN} \times 100 \tag{8}$$

$$Recall = \frac{TP}{TP+FN} \times 100 \tag{9}$$

$$Precision = \frac{TP}{TP+FP} \times 100 \tag{10}$$

$$F1-score = \frac{2 \times Precision \times Recall}{Precision+Recall} \times 100 \tag{11}$$

4.2. QUANTITATIVE EVALUATION IN TERMS OF SEGMENTATION

The proposed multi-resolution feature embedded level set model is tested and the obtained results are verified in terms of the IoU index. The segmentation results of the proposed multi-resolution feature embedded level set model are mentioned in Table 2 and Fig. 5. The original images with two crosshatched textures are acquired from Brodatz texture dataset, and their subjective boundaries are represented in Fig. 5(a). The histogram results of the original image are shown in Fig. 5(b), and the automated filter size selection of the developed algorithm is shown in Fig. 5(c). The segmentation results of the level set algorithm are shown in Fig. 5(d). Any noise encountered during the histogram process is eliminated by the operation of opening and closing the morphological image processing, as shown in Fig. 5(e). The selection of the filter size is very vital to perform proper segmentation in the original texture image. The algorithm initiates with a 3×3 filter size and then, increases the filter size until the size of the filter equals the mean of the image partition. If the above condition is satisfied, the value of the lower cluster is used as the filter size.

The segmented results are validated by using the IoU index value, which is presented in Table 2, wherein the reference IoU value is one. The IoU index of the image under study is greater than 0.9, which indicates that the proximity with the initial image is excellent, as shown in Table 2. The experimental outcome indicates that the proposed model is capable of segmenting the region of interest in close correspondence with the texture image. The proposed multi-resolution feature embedded level set model is compared with MixNCut [26]. The proposed segmentation model achieves precise accuracy on all the crosshatched texture images. It is measured by means of "raw" pixels that identify optimum segmentation. The proposed segmentation model significantly outperforms the existing segmentation model - MixNcut [26]. The experimental results of the proposed and the existing segmentation models, in terms of running time and IoU index, are shown in Table 2.

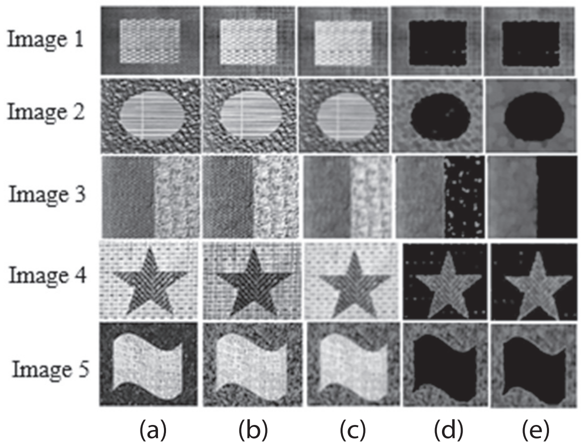

Fig. 5. Segmented output image (a) original image (Crosshatched) constructed from Brodatz texture dataset, b) histogram pre-processed image, (c) automated filter size selected by the proposed algorithm, (d) Segmented image through level set Algorithm, and (e) opening and closing results (Morphological Image Processing)

Table 2. Segmentation results in terms of IoU index value and running time

Index	Image 1		Image 2		Image 3		Image 4		Image 5	
Model	MixNcut [26]	Proposed	MixNcut [26]	Proposed	MixNcut [26]	Proposed	MixNcut [26]	Proposed	MixNcut [26]	Proposed
IoU	0.96	0.98	0.93	0.95	0.92	0.95	0.93	0.97	0.94	0.95
Time (sec)	9.09	6.30	6.61	5.42	7.15	5.35	8.05	5.72	7.89	5.81

4.2. QUANTITATIVE EVALUATION IN TERMS OF CLASSIFICATION

In the classification section, the proposed multi-resolution feature embedded level set model is tested with different classification techniques namely: random forest, K-Nearest Neighbor (KNN), Support Vector Machine (SVM), and Multi-SVM (MSVM) by means of f1-score, accuracy, precision, and recall with different cross fold validations: 5 and 10 folds. By inspecting Tables 3 and 4, it is seen that the combination of multi-resolution feature embedded level set model with histogram equalization and MSVM has obtained higher classification performance in five-fold cross-validation with f1-score of 98.90%, accuracy of 99.82%, precision of 99.12%, and recall of 98.88% on the Brodatz texture dataset. The graphical depiction of the proposed multi-resolution feature embedded level set model with different classifiers and testing percentages is shown in Fig. 6 and 7.

As seen in the comparative analysis in Table 5, the proposed multi-resolution feature embedded level set model with MSVM achieved comparatively higher classification results, when related to a model named modified CNN with WOA. The proposed model gained an f1-score of 98.90%, accuracy of 99.82%, precision of 99.12%, and recall of 98.88% on the Brodatz texture dataset. However, the modified CNN with WOA has obtained an accuracy of 99.71%, precision of 96.70%, recall of 95.80%, and f1-score of 96.20% on the Brodatz texture dataset. As depicted in the literature survey section, the proposed model effectively resolves the problems of higher computational time, and achieves better segmentation and classification performance.

Table 3. Experimental results of the proposed model with five-fold cross-validation (80:20% training and testing)

Classifiers	Without histogram equalization				With histogram equalization			
	F1-score (%)	Accuracy (%)	Precision (%)	Recall (%)	F1-score (%)	Accuracy (%)	Precision (%)	Recall (%)
Random forest	90.34	91.76	93.23	89.28	93.24	95.30	96.66	92.20
KNN	92.95	92.56	92.45	93.33	95.90	98.24	96.32	97
SVM	93.73	92.34	92.37	92.28	97.74	99.22	98.32	97.22
MSVM	94.34	93.43	92.10	92.90	98.90	99.82	99.12	98.88

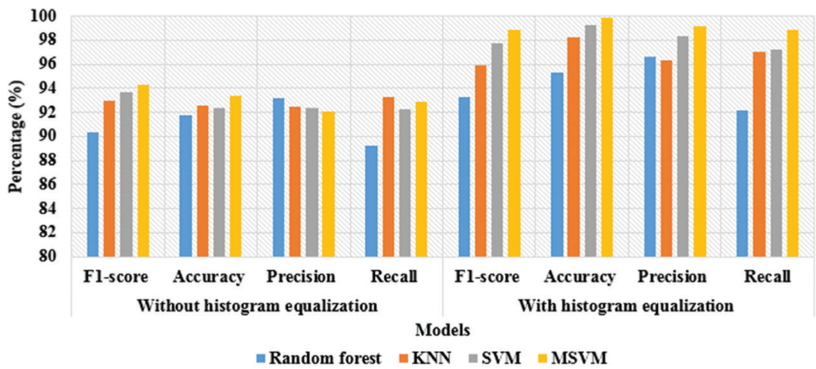

Fig. 6. Graphical depiction of the proposed model with five-fold cross-validation (80:20% training and testing)

Table 4. Experimental results of the proposed model with ten-fold cross-validation (90:10% training and testing)

Classifiers	Without histogram equalization				With histogram equalization			
	F1-score (%)	Accuracy (%)	Precision (%)	Recall (%)	F1-score (%)	Accuracy (%)	Precision (%)	Recall (%)
Random forest	88.12	90.43	91.13	84.24	92.20	94.38	93.62	90.28
KNN	90.44	90.55	91.15	90.34	92.90	94.28	93.34	94.07
SVM	92.66	91.55	90.36	87.99	93.79	95.20	95.35	94.25
MSVM	92.38	91.49	90.18	88.95	94.98	95.83	95.17	94.87

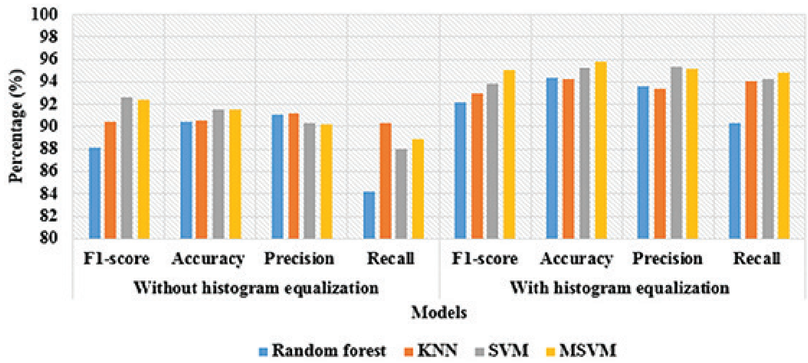

Fig. 7. Graphical depiction of the proposed model with ten-fold cross-validation (90:10% training and testing)

Table 5. Comparative results between the proposed and the existing models

Models	F1-score (%)	Accuracy (%)	Precision (%)	Recall (%)
Modified CNN with WOA [20]	96.20	99.71	96.70	95.80
Multi-resolution feature embedded level set with MSVM	98.90	99.82	99.12	98.88

5. CONCLUSION

In image processing applications, the main pre-processing steps for object detection are image segmentation and shape detection. In this research article, an effective model is proposed for computing the appropriate features and automatic selection of filter size in context of unsupervised texture segmentation. The proposed model determines the minimum size of the filter for texture feature extraction in order to enhance discrimination and segmentation capabilities. In this study, a multi-resolution feature embedded level set model is introduced, that segments challenging images like cross-hatched texture images, which are acquired from the Brodatz texture dataset. The experimental results show that the proposed model provides longer-range interactions and captures the complex region appearances. The proposed segmentation model with MSVM classifier has achieved a classification accuracy of 99.82%, which is superior compared to other models. The proposed model is practical and robust, and it is employed for other dissimilar types of texture images in future work.

6. REFERENCES

[1] B. Pascal, N. Pustelnik, P. Abry, "Strongly convex optimization for joint fractal feature estimation and texture segmentation", Applied and Computational Harmonic Analysis, Vol. 54, 2021, pp. 303-322.

[2] S. Kinge, B. S. Rani, M. Sutaone, "Markov Random Field Based Color Texture Segmentation", International Journal of Recent Technology and Engineering, Vol. 8, No. 5, 2020, pp. 1055-1060.

[3] P.-P. Niu, L. Wang, X. Shen, Q. Wang, X.-Y. Wang, "Texture image segmentation using Vonn mixtures-based hidden Markov tree model and relative phase", Multimedia Tools and Applications, Vol. 79, No. 39-40, 2020, pp. 29799-29824.

[4] U. Barman, R. D. Choudhury, "Soil texture classification using multi class support vector machine", Information Processing in Agriculture, Vol. 7, No. 2, 2020, pp. 318-332.

[5] B. Wang, X. Yuan, X. Gao, X. Li, D. Tao, "A hybrid level set with semantic shape constraint for object segmentation", IEEE Transactions on Cybernetics, Vol. 49, No. 5, 2019, pp. 1558-1569.

[6] S. Aouat, I. Ait-hammi, I. Hamouchene, “A new approach for texture segmentation based on the Gray Level Co-occurrence Matrix”, Multimedia Tools and Applications, Vol. 80, No. 16, 2021, pp. 24027-24052.

[7] B. Hui, Y. Liu, J. Qiu, L. Cao, L. Ji, Z. He, “Study of texture segmentation and classification for grading small hepatocellular carcinoma based on CT images”, Tsinghua Science and Technology, Vol. 26, No. 2, 2021, pp. 199-207.

[8] T. Kavzoglu, H. Tonbul, “An experimental comparison of multi-resolution segmentation, SLIC and K-means clustering for object-based classification of VHR imagery”, International Journal of Remote Sensing, Vol. 39, No. 18, 2018, pp. 6020-6036.

[9] D. Hamill, D. Buscombe, J. M. Wheaton, “Alluvial substrate mapping by automated texture segmentation of recreational-grade side scan sonar imagery”, PloS one, Vol. 13, No. 3, 2018, p. e0194373.

[10] Y. Almakady, S. M. Mahmoodi, M. Bennett, “Gaussian Markov random fields-based features for volumetric texture segmentation”, Proceedings of the IEEE Conference on Multimedia Information Processing and Retrieval, San Jose, CA, USA, 28-30 March 2019, pp. 212-215.

[11] D. Chen, Q. Chen, F. Zhu, “Pixel-level texture segmentation based AV1 video compression”, Proceedings of the IEEE International Conference on Acoustics, Speech and Signal Processing, Brighton, UK, 12-17 May 2019, pp. 1622-1626.

[12] N. Borodinov, W.-Y. Tsai, V. V. Korolkov, N. Balke, S. V. Kalinin, O. S. Ovchinnikova, “Machine learning-based multidomain processing for texture-based image segmentation and analysis”, Applied Physics Letters, Vol. 116, No. 4, 2020, p. 044103.

[13] B. Pascal, S. Vaiter, N. Pustelnik, P. Abry, “Automated data-driven selection of the hyperparameters for total-variation-based texture segmentation”, Journal of Mathematical Imaging and Vision, Vol. 63, No. 7, 2021, pp. 923-952.

[14] S. Y. Idrissi, “An active contour model for texture image segmentation using Rényi divergence measure”, Mathematical Modelling and Analysis, Vol. 27, No. 3, 2022, pp. 429-451.

[15] P. Pawlus, R. Reizer, M. Wieczorowski, “Functional importance of surface texture parameters”, Materials, Vol. 14, No. 18, 2021, p. 5326.

[16] L. Davy, N. Pustelnik, P. Abry, “Combining dual-tree wavelet analysis and proximal optimization for anisotropic scalefree texture segmentation”, https://hal.science/hal-03864647 (accessed: 2022).

[17] Y. Kang, “Retinex Algorithm and Mathematical Methods Based Texture Detail Enhancement Method for Panoramic Images”, Mathematical Problems in Engineering, Vol. 2022, 2022, p. 6490393.

[18] M. Maskey, T. S. Newman, “On measuring and employing texture directionality for image classification”, Pattern Analysis and Applications, Vol. 24, No. 4, 2021, pp. 1649-1665.

[19] A. Ranganath, M. R. Senapati, P. K. Sahu, “Classification of textures using pixel range calculation method”, Proceedings of the International Conference on Computing, Communication, and Intelligent Systems, Greater Noida, India, 19-20 February 2021, pp. 652-657.

[20] U. Dixit, A. Mishra, A. Shukla, R. Tiwari, “Texture classification using convolutional neural network optimized with whale optimization algorithm”, SN Applied Sciences, Vol. 1, No. 6, 2019, p. 655.

[21] M. Hilal, A. S. Gaudêncio, P. G. Vaz, J. Cardoso, A. Humeau-Heurtier, “Colored texture analysis fuzzy entropy methods with a dermoscopic application”, Entropy, Vol. 24, No. 6, 2022, p. 831.

[22] G. M. Raja, M. Thaha, R. Latha, A. Karthikeyan, “Texture classification using optimized local ternary patterns with nonlinear diffusion as pre-processing”, Multimedia Tools and Applications, Vol. 79, No. 5-6, 2020, pp. 3831-3846.

[23] L. A. Soares, K. F. Côco, P. M. Ciarelli, E. O. T. Salles, “A class-independent texture-separation method based on a pixel-wise binary classification”, Sensors, Vol. 20, No. 18, 2020, p. 5432.

[24] M. J. Khan, M. A. Riaz, H. Shahid, M. S. Khan, Y. Amin, J. Loo, H. Tenhunen, “Texture representation through overlapped multi-oriented tri-scale local binary pattern”, IEEE Access, Vol. 7, 2019, pp. 66668-66679.

[25] Z. Pan, X. Wu, Z. Li, “Scale-adaptive local binary pattern for texture classification”, Multimedia Tools and Applications, Vol. 79, No. 9, 2020, pp. 5477-5500.

[26] Y. Feng, R. Guo, X. Shen, X. Zhang, “A measure for the evaluation of multi-focus image fusion at feature level”, Multimedia Tools and Applications, Vol. 81, No.13, 2022, pp. 18053-18071.

[27] A. Ranganath, M. R. Senapati, P. K. Sahu, “Estimating the fractal dimension of images using pixel range calculation technique”, The Visual Computer, Vol. 37, No. 3, 2021, pp. 635-650.

[28] A. Ranganath, M. R. Senapati, P. K. Sahu, “A novel pixel range calculation technique for texture classification”, Multimedia Tools and Applications, Vol. 81, No. 13, 2022, pp. 17639-17667.

[29] A. Ranganath, P. K. Sahu, M. R. Senapati, “A novel approach for detection of coronavirus disease from computed tomography scan images using the pivot distribution count method”, Computer Methods in Biomechanics and Biomedical Engineering: Imaging & Visualization, Vol. 10, No. 2, 2022, pp. 145-156.

[30] A. Ranganath, P. K. Sahu, M. R. Senapati, "Detection of COVID from Chest X-Ray Images using Pivot Distribution Count Method", Proceedings of the 8th International Conference on Signal Processing and Integrated Networks, Noida, India, 26-27 August 2021, pp. 373-378.